

SABR smiles for RFR caplets

preliminary draft

Sander Willems
NatWest Markets*

First version: April 3, 2020
This version: April 10, 2020

Abstract

We present a natural extension of the SABR model to price both backward and forward-looking RFR caplets in a post-Libor world. Forward-looking RFR caplets can be priced using the market standard approximations of Hagan et al. (2002). We provide closed-form effective SABR parameters for pricing backward-looking RFR caplets. These results are useful for smile interpolation and for analyzing backward and forward-looking smiles in normalized units.

1 Introduction

Following a speech by the Financial Conduct Authority in July 2017, it became apparent that Libor is expected to cease after end 2021. Regulators have actively pushed for the development of new interest rate benchmarks that are firmly anchored to actual transactions, rather than expert judgement of a handful of panel banks. These new benchmarks are generally referred to as RFRs, short for risk-free rates. We refer to them in this paper simply as overnight rates, since that is what they are based on. Libor is currently by far the most important interest rate benchmark. The transition away from Libor therefore has widespread consequences for financial products, see for example Henrard (2019a) for a quantitative finance perspective. We focus in this paper in particular on the consequences for interest rate caps and floors.

A standard Libor caplet pays the difference between a Libor rate and a strike rate with a floor at zero. The payment occurs at the end of the accrual period to which the Libor rate refers, while the Libor rate itself, and therefore the caplet's payoff, is already known at the start of the accrual period. In a post-Libor world, caplets will possibly exist in two different formats. The first one, which we refer to as the *backward-looking* caplet, replaces the Libor rate by the compounded overnight rate over the accrual period. This product is conceptually different from a Libor caplet, since its payoff is only known at the end of the accrual period. The second one, which we refer to as the *forward-looking* caplet, replaces the Libor rate by the par rate of a single-period Overnight Index Swap (OIS) over the accrual period. This one is conceptually

*The statements and opinions expressed in this article are my own and do not represent the views of NatWest Markets Plc, NatWest Markets N.V. (and/or any branches) and/or their affiliates.

similar to a Libor caplet, but it requires a reliable OIS rate benchmark to be developed.¹

A natural modelling approach when working with overnight rates is to specify dynamics for the short-rate. Henrard (2004, 2006, 2019b) and Turfus (2020) derive explicit formulas for pricing backward-looking caplets in a single factor Gaussian short-rate model. These type of models however fail to produce a smile and can therefore only be calibrated to at-the-money caplets. This limits their practical use for traders. Macrina and Skovmand (2020) work with a linear-rational framework, similar to the framework in Filipović and Willems (2019), and rely on affine transforms to obtain semi-closed form solutions for backward-looking caplet prices. In a seminal contribution, Lyashenko and Mercurio (2019) extend the Libor Market Model (LMM) for use with compounded overnight rates, which they refer to as the Forward Market Model (FMM). They provide explicit formulas for backward-looking caplets for the lognormal case with constant volatility, which again does not produce a smile. The FMM framework is however much more general and allows in particular for stochastic volatility dynamics as well, although calibration can prove difficult if analytic solutions for backward-looking caplet prices are not available.

In this paper we propose an extension of the SABR model introduced by Hagan et al. (2002). Similarly as in Lyashenko and Mercurio (2019), we specify dynamics for the forward value of the compounded overnight rate over a certain accrual period. Before entering the accrual period, this rate follows standard SABR dynamics. Forward-looking caplets, whose payoff is known at the start of the accrual period, can therefore be priced using the market standard implied volatility approximation of Hagan et al. (2002). Once the rate enters the accrual period, it keeps evolving stochastically but its volatility is gradually scaled down to account for already realized overnight fixings. We build on the results of Hagan et al. (2018b) to derive effective constant SABR parameters that account for this time-dependent volatility scaling in the accrual period. Backward-looking caplets, which expire at the end of the accrual period, can therefore again be priced using the implied volatility approximation of Hagan et al. (2002), but with different parameters than forward-looking caplets. Our results allow traders to think of backward and forward-looking smiles in the same units, since we can map forward-looking SABR parameters into backward-looking ones and vice versa. Piterbarg (2020) highlights the importance of such an exercise and derives himself a correction to the initial volatility parameter in the SABR model, leaving the smile parameters unchanged. We show that this is indeed an important parameter to make an adjustment for in order to price the at-the-money backward-looking caplet correctly. For strikes away from the money, we show that an adjustment to the volatility-of-volatility parameter is important as well, in particular if we are close to or already in the accrual period.

The remaining of this paper is structured as follows. Section 2 describes the payoff of backward and forward-looking caplets. Section 3 introduces the backward-looking SABR model. Section 4 derives effective SABR parameters, which is the main contribution of this paper. Section 5 contains a numerical study of the new model. Section 6 concludes.

¹In January 2020, the ICE Benchmark Administration launched a market consultation on the introduction of an ICE swap rate based on SONIA, see ICE Benchmark Administration (2020).

2 Caplets in a post-Libor world

Consider two times $\tau_0 < \tau_1$ and define the continuously² compounded overnight rate as

$$R = \frac{1}{\tau_1 - \tau_0} \left(e^{\int_{\tau_0}^{\tau_1} r(s) ds} - 1 \right), \quad (1)$$

where $r(t)$ denotes an instantaneous proxy of the overnight rate. We define for $t \leq \tau_1$

$$R(t) = \mathbb{E}_t^{\tau_1}[R], \quad (2)$$

where $\mathbb{E}_t^{\tau_1}[\cdot]$ denotes the \mathcal{F}_t -conditional expectation with respect to the τ_1 -forward measure. In other words, a swap exchanging a floating payment R at τ_1 against a fixed payment K will have zero value at time t if $K = R(t)$. Note that $R(\tau_1) = R$, since the random variable R is \mathcal{F}_{τ_1} -measurable.

In a post-Libor world, there will possibly be two types of caplets. The first type, which we refer to as the backward-looking caplet, pays at time τ_1

$$V_{cpl}^b(\tau_1) = (R(\tau_1) - K)^+, \quad (3)$$

where K is the strike rate. This payoff is only known at payment time τ_1 . The second type, which we refer to as the forward-looking caplet, pays at time τ_1

$$V_{cpl}^f(\tau_1) = (R(\tau_0) - K)^+. \quad (4)$$

The payoff of the forward-looking caplet is already known at time τ_0 , but only paid at time τ_1 . The forward-looking caplet is therefore very similar to a traditional Libor caplet and equivalent to a single-period OIS swaption (see Remark 2.1). The value at time $t \leq \tau_1$ of the backward and forward-looking caplets are respectively given by:

$$V_{cpl}^b(t) = P(t, \tau_1) \mathbb{E}_t^{\tau_1}[(R(\tau_1) - K)^+], \quad (5)$$

$$V_{cpl}^f(t) = P(t, \tau_1) \mathbb{E}_t^{\tau_1}[(R(\tau_0) - K)^+], \quad (6)$$

where $P(t, \tau_1)$ denotes the price at time t of a zero-coupon bond with maturity τ_1 .

From Jensen's inequality, we get for $t \leq \tau_0$

$$V_{cpl}^f(t) \leq P(t, \tau_1) \mathbb{E}_t^{\tau_1} [\mathbb{E}_{\tau_0}^{\tau_1} [(R(\tau_1) - K)^+]] = V_{cpl}^b(t). \quad (7)$$

Therefore, the backward-looking caplet is always worth at least as much as the forward-looking caplet, provided we have not yet entered the accrual period. The above inequality has been highlighted by several authors, e.g., Lyashenko and Mercurio (2019), Dorn et al. (2019), and Piterbarg (2020). Note that we have equality in (7) if and only if interest rates are deterministic.

Remark 2.1. *By changing to the τ_0 -forward measure, we can express the value at time $t \leq \tau_0$ of the forward-looking caplet as*

$$V_{cpl}^f(t) = P(t, \tau_1) \mathbb{E}_t^{\tau_1}[(R(\tau_0) - K)^+] \quad (8)$$

$$= P(t, \tau_0) \mathbb{E}_t^{\tau_0}[P(\tau_0, \tau_1)(R(\tau_0) - K)^+]. \quad (9)$$

²In practice, overnight rates are compounded discretely on a daily basis, rather than continuously. For the purpose of this paper, however, this distinction is only of minor importance.

Note that $P(\tau_0, \tau_1)(R(\tau_0) - K)$ corresponds to the value at time τ_0 of a spot starting single-period OIS exchanging at time τ_1 a floating payment $R = R(\tau_1)$ against a fixed payment K . Therefore, the forward-looking caplet and the single-period OIS swaption have identical present values at time $t \leq \tau_0$. Note that this is not true for the backward-looking caplet.

3 Backward-looking SABR model

In this section we specify dynamics for $R(t)$. Before writing down the explicit equations, it is instructive to see what dynamics are implied from a simple short-rate model. Specifically, consider the following short-rate model

$$dr(t) = \xi(t) dB(t), \quad (10)$$

where $\xi(t)$ is some unspecified³ stochastic volatility process and $B(t)$ is a standard \mathbb{Q}^{τ_1} -Brownian motion.⁴ Using the first order approximation

$$R \approx \frac{1}{\tau_1 - \tau_0} \int_{\tau_0}^{\tau_1} r(s) ds, \quad (11)$$

we get together with (2) the following approximation

$$R(t) \approx \begin{cases} r(t), & t \leq \tau_0, \\ \frac{\int_{\tau_0}^t r(s) ds + r(t)(\tau_1 - t)}{\tau_1 - \tau_0}, & \tau_0 < t \leq \tau_1. \end{cases} \quad (12)$$

Applying Itô's lemma, we obtain the following approximate dynamics for $R(t)$:

$$dR(t) \approx \psi(t)\xi(t) dB(t), \quad \psi(t) = \min\left(1, \frac{\tau_1 - t}{\tau_1 - \tau_0}\right). \quad (13)$$

For $t \leq \tau_0$, the dynamics are the same as that of $r(t)$ and for $t \geq \tau_0$ the volatility is scaled by a function that decays linearly towards zero as $t \rightarrow \tau_1$. The decreasing volatility for $\tau_0 \leq t \leq \tau_1$ is of course not surprising, since an increasing part of the integral $\int_{\tau_0}^{\tau_1} r(s) ds$ is realised as time moves through the accrual period $[\tau_0, \tau_1]$. Similar observations have been made by Lyashenko and Mercurio (2019) and Piterbarg (2020).

From its definition (2), we require $R(t)$ to be a \mathbb{Q}^{τ_1} -martingale. The above considerations now motivate the following definition for the dynamics of $R(t)$:

$$dR(t) = \psi(t)R(t)^\beta \sigma(t) dB(t) \quad (14)$$

$$d\sigma(t) = \nu\sigma(t) dW(t), \quad \sigma(0) = \alpha, \quad (15)$$

with $\beta \in [0, 1]$, $\alpha, \nu > 0$, and $B(t), W(t)$ two \mathbb{Q}^{τ_1} -Brownian motions with $dB(t) dW(t) = \rho dt$, $\rho \in [-1, 1]$.⁵ For $t \leq \tau_0$, $R(t)$ follows standard SABR dynamics. For $t \geq \tau_0$, the stochastic

³We assume that $\xi(t)$ is such that the stochastic integral is well defined, but otherwise no assumptions are made.

⁴Note that $r(t)$ does not necessarily have to be a martingale under \mathbb{Q}^{τ_1} . This specification of $r(t)$ is simply a heuristic to gain some insight in the dynamics of $R(t)$ for $t > \tau_0$.

⁵We assume a zero lower bound for $R(t)$, however it is straightforward to accommodate an arbitrary lower bound through a displacement.

volatility process is scaled in the same way as in (13). Pricing forward-looking caplets, i.e. options on $R(\tau_0)$, can be done easily using the implied volatility approximations of Hagan et al. (2002):

$$V_{cpl}^f(0) = P(0, \tau_1) \text{Black} \left(\tau_0, K, R(0), \sigma_{IV}^f \right), \quad (16)$$

$$\sigma_{IV}^f \approx \sigma_{hagan}(\tau_0, K, R(0), \alpha, \beta, \rho, \nu), \quad (17)$$

where $\text{Black}(\dots)$ denotes Black (1976)'s formula and $\sigma_{hagan}(\dots)$ denotes the Black implied volatility approximation of Hagan et al. (2002).⁶ Pricing backward-looking caplets, i.e. options on $R(\tau_1)$, is more involved because of the time dependence through the function $\psi(t)$. In the next section we derive effective SABR parameters $\hat{\alpha}$, $\hat{\rho}$, $\hat{\nu}$ such that

$$V_{cpl}^b(0) = P(0, \tau_1) \text{Black} \left(\tau_1, K, R(0), \sigma_{IV}^b \right), \quad (18)$$

$$\sigma_{IV}^b \approx \sigma_{hagan}(\tau_1, K, R(0), \hat{\alpha}, \hat{\rho}, \hat{\nu}). \quad (19)$$

Note the difference between (16)-(17) and (18)-(19) in the time-to-exercise parameter, which reflects the fact that the forward-looking rate fixes at τ_0 while the backward-looking rate fixes at τ_1 . Also note that no additional treatment is required for pricing a backward-looking caplet with $\tau_0 < 0$, i.e. when some of the rate fixings in the payoff have already realized.

Remark 3.1. *The dynamics in (14)-(15) are in fact a special case of the general FMM model introduced by Lyashenko and Mercurio (2019) for once specific tenor. Our results can therefore be used to construct a SABR style FMM model with analytic prices for both backward and forward-looking caplets.*

4 Backward-looking effective SABR parameters

We apply the results of Hagan et al. (2018b) to find effective SABR parameters $\hat{\alpha}$, $\hat{\rho}$, $\hat{\nu}$ for the model in (14)-(15). Their results, based on singular perturbation techniques and effective medium theory, are not exact but have the same accuracy as the original SABR approximation of Hagan et al. (2002). We distinguish two cases, based on the sign of τ_0 .

If $\tau_0 < 0$, then part of the backward-looking caplet's payoff has realized already. In this case $\psi(t)$ is strictly decreasing towards zero as time moves forward, which decreases the volatility of $R(t)$. The following theorem presents effective SABR parameters that incorporate this time-dependent volatility scaling:

Theorem 4.1. *If $\tau_0 \leq 0$, then the backward-looking effective SABR parameters are*

$$\hat{\rho} = \rho \left(\frac{25}{28} + \frac{3}{14} \rho^2 \right)^{-\frac{1}{2}}, \quad (20)$$

$$\hat{\nu} = \nu \left(\frac{3}{7} + \frac{18}{175} \rho^2 \right)^{\frac{1}{2}}, \quad (21)$$

$$\hat{\alpha} = \frac{\alpha}{\sqrt{3}} \frac{\tau_1}{\tau_1 - \tau_0} e^{\frac{1}{8}(\nu^2 - 2\hat{\nu}^2)\tau_1}. \quad (22)$$

⁶Remark that (16)-(17) only makes sense for $\tau_0 > 0$. For $\tau_0 \leq 0$, we have $V_{cpl}^f(0) = P(0, \tau_1)(R(\tau_0) - K)^+$.

Proof. See Appendix. □

Remark that the effective smile parameters $\hat{\rho}$ and $\hat{\nu}$ do not depend on the length of the accrual period, nor on how far we are in already. The effective correlation does not change much, for example for $\rho = 50\%$ we have $\hat{\rho} = 51\%$. The effective volatility of volatility on the other hand is reduced substantially. For example, for $\nu = 20\%$ and $\rho = 50\%$, we have $\hat{\nu} = 13\%$. The behaviour of the effective initial volatility $\hat{\alpha}$ is slightly more involved. The exponential factor in (22) is a second order correction and does not contribute much. At the start of the accrual period, i.e. when $\tau_0 = 0$, $\hat{\alpha}^2$ is roughly one third of α^2 . As we move through the accrual period, $\hat{\alpha}$ gradually decreases towards zero, which reflects the fact that an increasing part of the compounded overnight rate has realized already.

If $\tau_0 \geq 0$, then none of the rates referenced in the backward-looking caplet's payoff have been realized yet. The rate $R(t)$ follows standard SABR dynamics until time τ_0 , and only afterwards will the volatility process be scaled down towards zero as $t \rightarrow \tau_1$. The following theorem provides the effective SABR parameters in this case.

Theorem 4.2. *If $\tau_0 \geq 0$, then the backward-looking effective SABR parameters are*

$$\hat{\rho} = \rho \frac{7\tau_0^2 + 6\tau_1\tau_0 + 2\tau_1^2}{15\sqrt{\gamma}}, \quad (23)$$

$$\hat{\nu} = \nu \left(\frac{\gamma}{\tau^3\tau_1} \right)^{\frac{1}{2}}, \quad (24)$$

$$\hat{\alpha} = \alpha \left(\frac{\tau}{\tau_1} \right)^{\frac{1}{2}} e^{\frac{1}{8}H\tau_1}, \quad (25)$$

where we have defined the following constants

$$\begin{aligned} \tau &= \frac{2}{3}\tau_0 + \frac{1}{3}\tau_1, \quad H = \nu^2 \frac{\tau_1^2 + 2\tau_1\tau_0 + 3\tau_0^2}{3\tau_1\tau} - 2\hat{\nu}^2, \\ \gamma &= \frac{1}{21} \left[\tau(\tau_1^3 + 4\tau_1^2\tau_0 + 10\tau_1\tau_0^2 + 6\tau_0^3) + \frac{\rho^2}{25}(\tau_1 - \tau_0)^2(2\tau_1^2 + 16\tau_1\tau_0 + 17\tau_0^2) \right] \end{aligned}$$

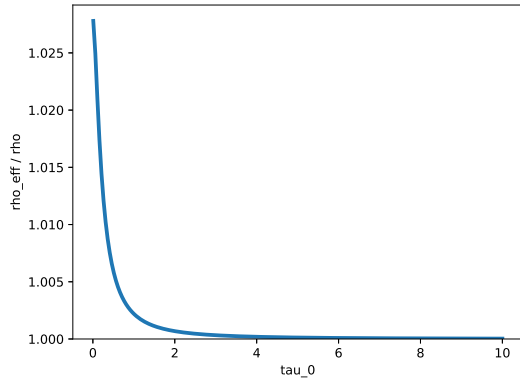
Proof. See Appendix. □

For $\tau_0 = 0$, Theorem 4.1 and 4.2 agree. For $\tau_1 = \tau_0 > 0$, the backward-looking SABR model reduces to the standard SABR model and Theorem 4.2 indeed gives in this case $\hat{\rho} = \rho$, $\hat{\nu} = \nu$, and $\hat{\alpha} = \alpha$. In Figure 1, we fix the length of the accrual period to $\tau_1 - \tau_0 = 0.5$ and plot the impact of changing τ_0 on the ratios $\hat{\rho}/\rho$, $\hat{\nu}/\nu$, and $\hat{\alpha}/\alpha$. We observe that the impact is strongest for τ_0 close to zero and becomes less noticeable for larger τ_0 . This makes sense intuitively, since for large τ_0 , the model behaves like a regular SABR model most of the time.

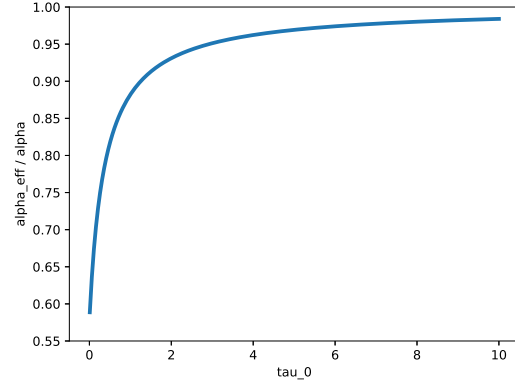
Remark 4.3. *Piterbarg (2020) derives for $\tau_0 > 0$ an adjusted initial volatility $\tilde{\alpha}$ such that*

$$V_{cpl}^b(0) = P(0, \tau_1) \text{Black}(\tau_0, K, R(0), \tilde{\sigma}_{IV}^b), \quad (26)$$

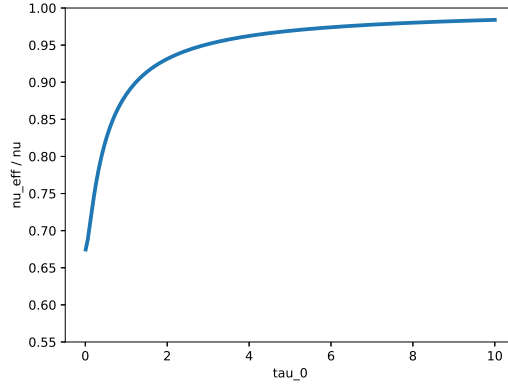
$$\tilde{\sigma}_{IV}^b = \sigma_{hagan}(\tau_0, K, R(0), \tilde{\alpha}, \beta, \rho, \nu). \quad (27)$$



(a) $\hat{\rho}/\rho$



(b) $\hat{\alpha}/\alpha$



(c) $\hat{\nu}/\nu$

Figure 1: Ratio of effective SABR parameter over original one as a function of τ_0 . The length of the accrual period is set to $\tau_1 - \tau_0 = 0.5$.

Note that the effective parameters $\hat{\alpha}, \hat{\rho}, \hat{\nu}$ in (18)-(19) correspond to a time-to-exercise τ_1 , while $\tilde{\alpha}$ corresponds to a time-to-exercise τ_0 .⁷ In order to compare $\hat{\alpha}$ with $\tilde{\alpha}$, we scale $\hat{\alpha}$ by $\sqrt{\frac{\tau_1}{\tau_0}}$:

$$\hat{\alpha}\sqrt{\frac{\tau_1}{\tau_0}} = \alpha\sqrt{\frac{2}{3}\tau_0 + \frac{1}{3}\tau_1}e^{\frac{1}{8}H\tau_1} = \alpha\sqrt{1 + \frac{\tau_1 - \tau_0}{3\tau_0}}e^{\frac{1}{8}H\tau_1}. \quad (28)$$

Ignoring the exponential factor, which is typically very close to one, the right-hand side in (28) agrees with the adjusted initial volatility $\tilde{\alpha}$ derived by Piterbarg (2020).

5 Numerical study

In order to evaluate the approximation quality of the effective SABR parameters derived in the previous section, we perform a Monte-Carlo simulation of the model as a benchmark. We arbitrarily choose the following parameter values: $\beta = 1$, $R(0) = 0.05$, $\tau_0 = 0.5$, $\tau_1 = 1$, $\rho = -0.50$, $\nu = 0.50$, $\alpha = 0.10$. The effective parameters, computed using Theorem 4.2, become

$$\hat{\alpha} = 0.082, \quad \hat{\rho} = -0.503, \quad \hat{\nu} = 0.411.$$

We simulate (14)-(15) using a log-Euler discretization scheme with time step $1/512$ and 10^6 simulation trajectories. Figure 2 shows an example of three simulated trajectories of $R(t)$. Notice how the volatility starts to decrease for $t > \tau_0$. We use the simulated trajectories to price backward-looking caplets and then compute Black implied volatility by inverting Black (1976)'s formula. Figure 3 shows that Hagan et al. (2002)'s implied volatility approximation with effective parameters $\hat{\alpha}, \hat{\rho}, \hat{\nu}$ produces virtually identical results as the Monte-Carlo simulation. As a reference, we also plot implied volatilities computed using Hagan et al. (2002)'s approximation with parameters α, ρ, ν and $\hat{\alpha}, \rho, \nu$. In the first case, we do not apply any adjustments to the SABR parameters, and Figure 3 clearly shows we are substantially mispricing caplets at all strikes. In the second case, we only apply a correction to the initial volatility parameter, in a similar spirit as the correction proposed in Piterbarg (2020). The at-the-money strike is priced correctly in this case, but strikes away from the money are not.

6 Conclusion

We have presented a natural extension of the SABR model to consistently price backward and forward-looking caplets. Forward-looking caplets can be priced using the market standard approximations of Hagan et al. (2002). Building on the results of Hagan et al. (2018b), we have derived closed-form effective SABR parameters for pricing backward-looking caplets. We have shown the effective SABR approximation to be highly accurate when compared to a Monte-Carlo simulation benchmark. The correction to the initial volatility and the volatility-of-volatility parameters are most pronounced, while the correction to the correlation parameter is of second order importance. Our results allow traders to think of backward and forward-looking caplets in normalized units, which helps to assess their relative values. A similar analysis can be done for the Heston (1993) model using, for example, the results from Hagan et al. (2018a). We leave such extensions for future research.

⁷The advantage of working with time-to-exercise τ_1 is that it allows to deal with $\tau_0 \leq 0$ as well.

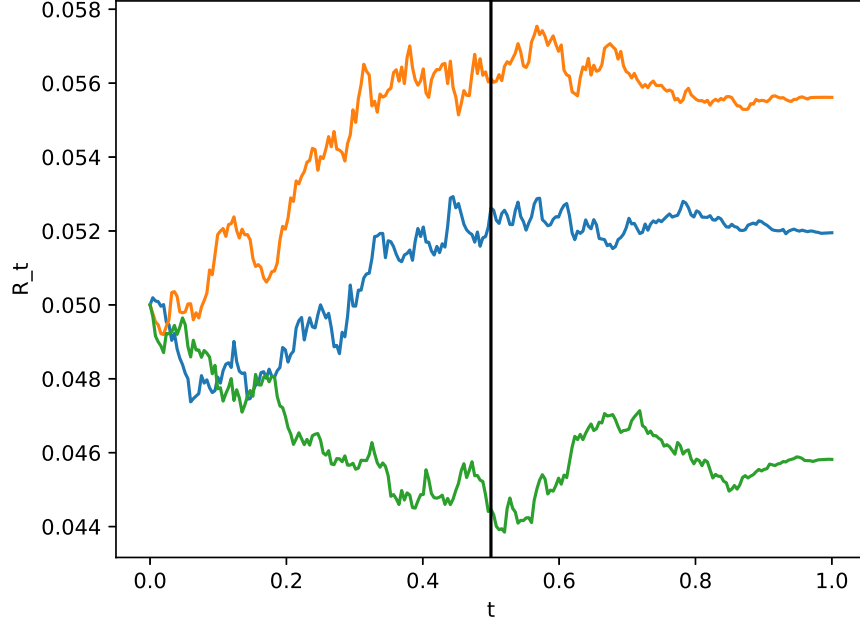


Figure 2: Three simulated trajectories of $R(t)$. The vertical black line indicates the start of the accrual period $t = \tau_0$.

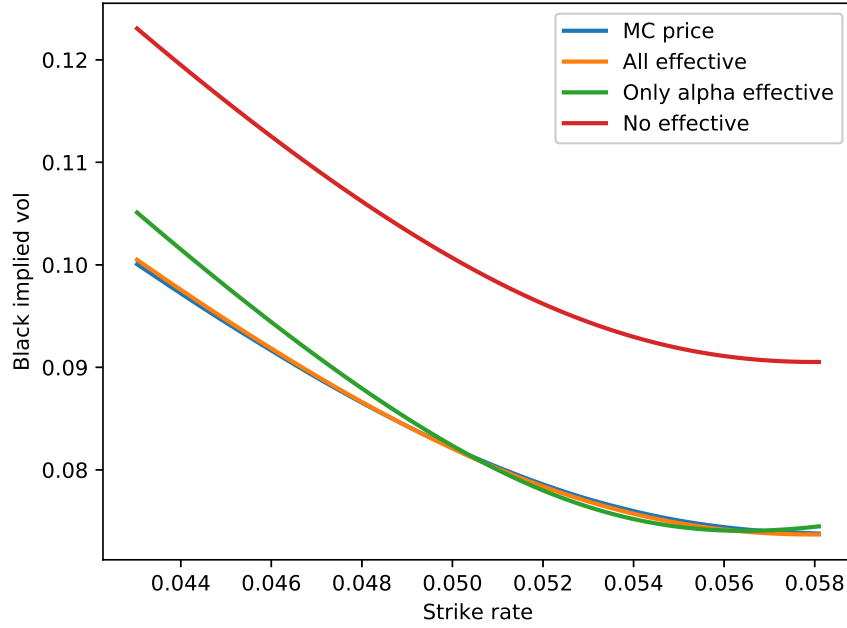


Figure 3: Black implied volatility smiles. The blue line corresponds to the Monte-Carlo price, the orange line to the SABR price with $(\hat{\alpha}, \hat{\rho}, \hat{\nu})$, the green line to SABR price with $(\hat{\alpha}, \rho, \nu)$, and the red line to the SABR price with (α, ρ, ν) .

A Proofs

A.1 Proof of Theorem 4.1

We start by summarizing a particular case of the results in Hagan et al. (2018b).

Theorem A.1 (Hagan et al. (2018b)). *Consider for $\epsilon > 0$ the following dynamics*

$$dR_\epsilon(t) = \epsilon \phi(t) R_\epsilon(t)^\beta \sigma_\epsilon(t) dB(t) \quad (29)$$

$$d\sigma_\epsilon(t) = \epsilon \nu \sigma_\epsilon(t) dW(t), \quad \sigma_\epsilon(0) = 1. \quad (30)$$

For a given expiry $T > 0$, Hagan et al. (2018b) show that to within $\mathcal{O}(\epsilon^2)$, the implied volatility of European options under the model in (29)-(30) coincides with the implied volatility under the standard SABR model with constant parameters

$$\hat{\alpha} = \Delta e^{\frac{1}{4}\epsilon^2 \Delta^2 GT}, \quad \hat{\rho} = \frac{b}{\sqrt{c}}, \quad \hat{\nu} = \Delta \sqrt{c},$$

where the following constants are defined

$$\begin{aligned} \Delta^2 &= \frac{v(T)}{T}, \quad b = \frac{2\rho\nu}{v^2(T)} \int_0^T (v(T) - v(s))\phi(s) ds, \quad G = \frac{2\nu^2}{v^2(T)} \int_0^T v(T) - v(s) ds - c, \\ c &= \frac{3\nu^2}{v^3(T)} \int_0^T (v(T) - v(s))^2 ds + \frac{9}{v^3(T)} \int_0^T w^2(s)\phi^2(s) ds - 3b^2, \end{aligned}$$

with $v: u \mapsto \int_0^u \phi^2(s) ds$, and $w: u \mapsto \rho\nu \int_0^u \phi(s) ds$.

Note that the accuracy of the original SABR approximation in Hagan et al. (2002) was also of the order $\mathcal{O}(\epsilon^2)$. The accuracy of the effective parameter approximation is therefore of the same order as the original approximation.

We can apply the above result to the backward-looking SABR model in (14)-(15) by setting $\epsilon = 1$, $\phi(t) = \alpha\psi(t)$, and $T = \tau_1$. For $\tau_0 < 0$, we have therefore

$$\phi(t) = \alpha \frac{\tau_1 - t}{\tau_1 - \tau_0}, \quad t \leq \tau_1.$$

It remains to calculate the integrals appearing in Theorem A.1. We start with the functions v and w :

$$\begin{aligned} v(u) &= \frac{\alpha^2}{\tau_1 - \tau_0} \int_0^u (\tau_1 - s)^2 ds = \alpha^2 \frac{\tau_1^3 - (\tau_1 - u)^3}{3(\tau_1 - \tau_0)^2}, \\ w(u) &= \frac{\rho\nu}{\tau_1 - \tau_0} \int_0^u (\tau_1 - s) ds = \rho\nu\alpha \frac{\tau_1^2 - (\tau_1 - u)^2}{2(\tau_1 - \tau_0)}. \end{aligned}$$

In particular, we have $v(\tau_1) = \alpha^2 \frac{\tau_1^3}{3(\tau_1 - \tau_0)^2}$ and $v(\tau_1) - v(s) = \alpha^2 \frac{(\tau_1 - s)^3}{3(\tau_1 - \tau_0)^2}$. Elementary, but rather tedious, calculations give

$$\begin{aligned} b &= \frac{6}{5} \frac{\rho\nu}{\alpha} \frac{\tau_1 - \tau_0}{\tau_1}, \quad c = \frac{\nu^2}{\alpha^2} \frac{(\tau_1 - \tau_0)^2}{\tau_1^2} \left(\frac{9}{7} + \frac{54}{175} \rho^2 \right), \\ \Delta &= \frac{\alpha}{\sqrt{3}} \frac{\tau_1}{\tau_1 - \tau_0}, \quad G = \frac{\nu^2}{\Delta^2} \left(\frac{1}{14} - \frac{18}{175} \rho^2 \right). \end{aligned}$$

Putting things together gives

$$\begin{aligned}\hat{\alpha}^2 &= \Delta^2 e^{\frac{1}{2}\Delta^2 G \tau_1} = \frac{\alpha^2}{3} \frac{\tau_1^2}{(\tau_1 - \tau_0)^2} e^{\frac{1}{2}\nu^2(\frac{1}{14} - \frac{18}{175}\rho^2)\tau_1}, \\ \hat{\nu}^2 &= \Delta^2 c = \nu^2 \left(\frac{3}{7} + \rho^2 \frac{18}{175} \right), \\ \hat{\rho} &= \frac{b}{\sqrt{c}} = \frac{\frac{6}{5} \frac{\rho\nu}{\alpha} \frac{\tau_1 - \tau_0}{\tau_1}}{\frac{\nu}{\alpha} \frac{\tau_1 - \tau_0}{\tau_1} \sqrt{\frac{9}{7} + \frac{54}{175}\rho^2}} = \frac{2}{5} \rho \left(\frac{1}{7} + \frac{6}{175}\rho^2 \right)^{-\frac{1}{2}}\end{aligned}$$

This proves the theorem.

A.2 Proof of Theorem 4.2

Similarly as in the proof of Theorem 4.1, we again apply Theorem A.1 with $\epsilon = 1$, $\phi(t) = \alpha\psi(t)$, and $T = \tau_1$. For the case $\tau_0 \geq 0$ we get

$$\phi(t) = \begin{cases} \alpha, & 0 \leq t \leq \tau_0, \\ \alpha \frac{\tau_1 - t}{\tau_1 - \tau_0}, & \tau_0 \leq t \leq \tau_1. \end{cases}$$

The functions v and w become:

$$\begin{aligned}v(u) &= \begin{cases} \alpha^2 u, & 0 \leq u \leq \tau_0, \\ \frac{\alpha^2}{3} \left(2\tau_0 + \tau_1 - \frac{(\tau_1 - u)^3}{(\tau_1 - \tau_0)^2} \right), & \tau_0 \leq u \leq \tau_1, \end{cases} \\ w(u) &= \begin{cases} \rho\nu\alpha u, & 0 \leq u \leq \tau_0, \\ \frac{\rho\nu\alpha}{2} \left(\tau_0 + \tau_1 - \frac{(\tau_1 - u)^2}{\tau_1 - \tau_0} \right), & \tau_0 \leq u \leq \tau_1. \end{cases}\end{aligned}$$

Elementary, but rather tedious, calculations give

$$\begin{aligned}b &= \frac{3\rho\nu(7\tau_0^2 + 6\tau_1\tau_0 + 2\tau_1^2)}{5\alpha(2\tau_0 + \tau_1)^2}, \quad c = \frac{81\nu^2\gamma}{\alpha^2(2\tau_0 + \tau_1)^4}, \quad \Delta = \alpha\sqrt{\frac{2\tau_0 + \tau_1}{3\tau_1}}, \\ \gamma &= \frac{1}{21} \left(\frac{1}{3}(2\tau_0 + \tau_1)(\tau_1^3 + 4\tau_1^2\tau_0 + 10\tau_1\tau_0^2 + 6\tau_0^3) + \frac{1}{25}\rho^2(\tau_1 - \tau_0)^2(2T^2 + 16\tau_1\tau_0 + 17\tau_0^2) \right), \\ G &= \frac{3\nu^2(\tau_1^2 + 2\tau_1\tau_0 + 3\tau_0^2)}{2\alpha^2(2\tau_0 + \tau_1)^2} - c.\end{aligned}$$

Putting things together gives

$$\begin{aligned}\hat{\alpha}^2 &= \Delta^2 e^{\frac{1}{2}\Delta^2 G \tau_1} = \alpha^2 \frac{1}{\tau_1} \left(\frac{2}{3}\tau_0 + \frac{1}{3}\tau_1 \right) e^{\frac{1}{2}\Delta^2 G \tau_1}, \\ \hat{\nu}^2 &= \Delta^2 c = \frac{\nu^2\gamma}{\tau_1(\frac{2}{3}\tau_0 + \frac{1}{3}\tau_1)^3}, \\ \hat{\rho} &= \frac{b}{\sqrt{c}} = \rho \frac{7\tau_0^2 + 6\tau_1\tau_0 + 2\tau_1^2}{15\sqrt{\gamma}}.\end{aligned}$$

Substituting $H = 2\Delta^2 G$ concludes the proof.

References

- Black, F. (1976). The pricing of commodity contracts. *Journal of Financial Economics* 3(1-2), 167–179.
- Dorn, J., D. Filipovic, S. Pomberger, and S. Willems (2019). Back to a single curve? State of play of alternative risk-free rates. *QuantMinds International presentation*.
- Filipović, D. and S. Willems (2019). A term structure model for dividends and interest rates. *Swiss Finance Institute Research Paper* (17-52).
- Hagan, P. S., D. Kumar, A. S. Lesniewski, and D. E. Woodward (2002). Managing smile risk. *Wilmott Magazine*, 84–108.
- Hagan, P. S., A. S. Lesniewski, and D. E. Woodward (2018a). Implied volatility formulas for Heston models. *Wilmott Magazine* (98), 44–57.
- Hagan, P. S., A. S. Lesniewski, and D. E. Woodward (2018b). Managing vol surfaces. *Wilmott Magazine* (93), 24–43.
- Henrard, M. (2004). Overnight indexed swaps and floored compounded instrument in HJM one-factor model. *Working Paper*.
- Henrard, M. (2006). Skewed Libor market model and Gaussian HJM explicit approaches to rolled deposit options. *Available at SSRN 956849*.
- Henrard, M. (2019a). LIBOR fallback and quantitative finance. *Risks* 7(3), 88.
- Henrard, M. (2019b). A quant perspective on ibor fallback consultation results-v2. 1. *Market Infrastructure Analysis, muRisQ Advisory, January*.
- Heston, S. L. (1993). A closed-form solution for options with stochastic volatility with applications to bond and currency options. *The Review of Financial Studies* 6(2), 327–343.
- ICE Benchmark Administration (2020). Consultation on introduction of ICE Swap Rate based on SONIA. https://www.theice.com/publicdocs/Consultation_on_introduction_of_ICE_Swap_Rate_
- Lyashenko, A. and F. Mercurio (2019). Looking forward to backward-looking rates: A modeling framework for term rates replacing LIBOR. *Available at SSRN 3330240*.
- Macrina, A. and D. Skovmand (2020). Rational savings account models for backward-looking interest rate benchmarks. *Risks* 8(1), 23.
- Piterbarg, V. (2020). Interest rates benchmark reform and options markets. *Available at SSRN 3537925*.
- Turfus, C. (2020). Caplet pricing with backward-looking rates. *Available at SSRN 3527091*.